วิศวกรรมสาร ม.ข. ปีที่ 31 ฉบับที่ 4 (319-336) ตุลาคม - ธันวาคม 2547
KKU Engineering Journal Vol. 31 No. 4 (319-336) October –December 2004

Mixing Plate and Beam Elements in *FEAP*: A Plate Stiffened with Beams

Suchart Limkatanyu
Ph.D. (Structural Engineering); Lecturer Department of Civil Engineering, Faculty of Engineering, Prince of Songkla University, Hadyai, Songkhla, Thailand, 90112.

Abstract

This paper investigates the mixability of plate and beam elements in finite element meshes and is separated into three parts. The first part is a look at verifying if plate and beam elements could be intermixed in a general-purpose finite element program like *FEAP* in this study. The second part is a look at how well a finite element model of a simple plate with edge beams (using both shell and beam elements) could match the available analytical solutions. The third part investigates the similarities and differences encountered when modeling the plate with edge beams using either beam elements or shell elements to represent the beam-stiffeners. The model assessments are conducted both under static and dynamic analysis. The results indicate that *FEAP* handles the problem of mixing beam and plate elements excellently, and that beam elements can be used in place of shell element combinations, hence allowing both modeling and analyzing much faster as long as one pays attentions to the torsional characteristics of the beam profile.

Keywords: finite element, shell, plate, beam, mixability, stiffener, torsional stiffness, vibration.

Introduction

The main focus in this paper is on plates stiffened on the free edges with beam stiffeners. The shell and beam elements were used to represent the beam stiffener and the accuracy of the analysis was investigated. The analysis was performed with the general-purpose finite element program, *FEAP* (Taylor, 1998). In the research community, most of the studies on the stiffened plates have emphasized on the models where the stiffeners were smeared over the span of the plates and the spring stiffeners were placed along the edges (e.g. Laura and Romanelli, 1974 and Leissa et al., 1980). For comparison and verification of the proposed mixed mesh in this study, the analytical solutions developed by Timoshenko and Woinowsky-Krieger (1959) served as the benchmark solution. Timoshenko and Woinowsky-Krieger (1959) derived the analytical solutions for a plate with stiffeners on either two or four free edges, where in the former case, the other two edges are simply supported and in the latter case, the corners are pinned.

The two case studies mentioned above were performed under static condition, where uniform load was distributed over the plate and under dynamic condition, where eigen-modes resulting from eigen-values analysis were compared

between various kinds of beam cross-section profiles. Different profiles of the beams were also modeled using shell elements and are referred to in the paper as *"shell-beam"*. Profiles and configurations used in the study are: square-tube, C, uneven-C, Z, and offset I-beams.

Before performing any comparisons and analyses, it is necessary to conduct a patch test in order to validate the compatibility of the two different models used in the finite element mesh containing both plate and beam elements. The plate element used has five degree of freedoms (dofs) at each node: three for translations and two for bending rotations, thus lacking the in-plane twist (drilling dof). The beam element used is a classical Hermite 3D beam with six dofs at each node: three for translations and three for rotations.

Patch Test

Patch tests historically originated by Irons (Bazeley, Cheung, Irons, and Zienkiewicz, 1966) are performed to ensure that the 4-node plate element (Quad-4), having 5 dofs at each node is compatible with the 2-node beam element, having 6 dofs at each node (Figure 1).

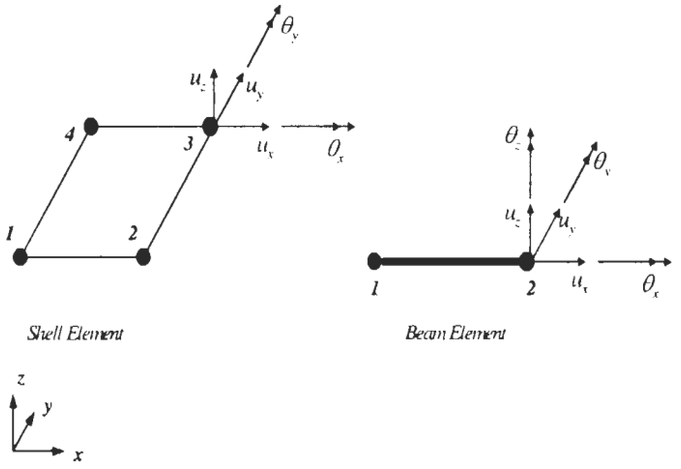

Figure 1 Shell and beam elements used in the analysis

Rigid Body Modes

Two translation tests and one rotation test are performed to ensure that the proposed mixed mesh contains appropriate rigid body modes. In the translation test, all external nodes are imposed a unit translation and it is verified that the center node shows the same translation. In the rotation test, a combination of translations is used to create a rotation of the whole patch (Figure 2). In translation tests, the center node displays exactly the same displacement as the external nodes as well as in the rotation test.

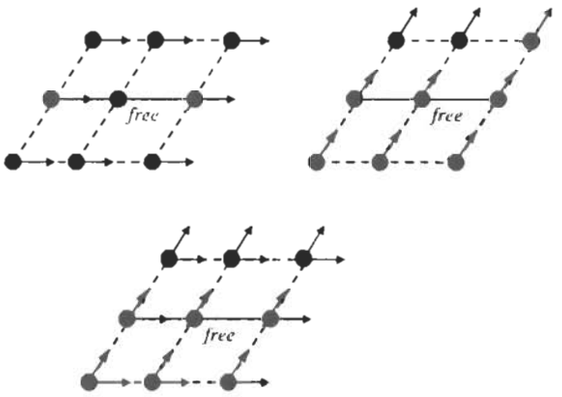

Figure 2 Unit displacement applied in x and y directions

Constant Stress Field

Herein a constant force per length is applied along the edge of the patch in order to create a constant stress field. It is verified that the FEAP program lumps the load correctly onto the three edge nodes as shown in Figure 3 and Figure 4 in the x and y directions, respectively.

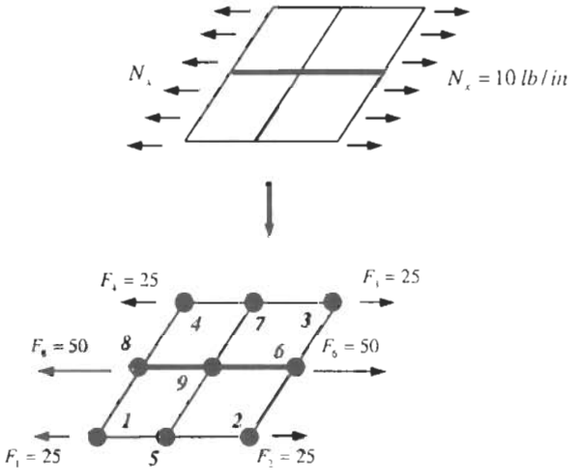

Figure 3 Constant stress applied *in x direction*

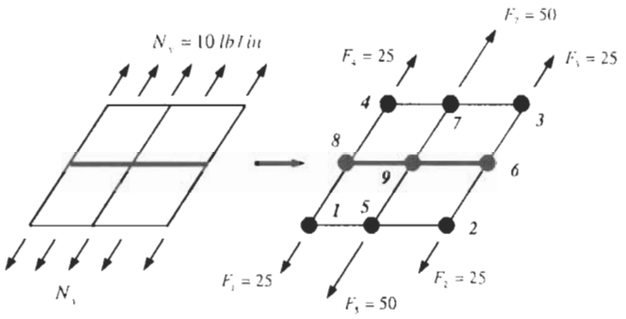

Figure 4 Constant stress applied in *y* direction

The formulas used to verify the compatibility are:

$$F_{xp} = \sigma_{xp} t_p H_p \tag{1}$$

$$F_{xb} = \sigma_{xb} A_b \tag{2}$$

$$N_x H_p = F_{xp} + F_{xb} \tag{3}$$

where F_{xp} = force contribution from plate; σ_{xp} = calculated plate stress from *FEAP* in the *x* direction; t_p = thickness of plate, 0.125 *in*; H_p = length of side where load is applied, 10 *in*; F_{xb} = force contribution from beam; σ_{xb} = calculated beam stress from *FEAP* in the *x* direction; A_b = cross-sectional area of beam, 0.25 in^2 ; and N_x = applied in-plane load, force per length, 10 lb/in.

Similar formulas apply for the constant stress in the *y* direction except that the beam has no node on the edge, where the load is applied, and therefore does not come into account when considering the loads there.

When a load N_x is applied as shown in Figure 3, the stresses in the *x* direction are $\sigma_{xp} = 69.75$ psi and $\sigma_{xb} = 51.25$ psi therefore $F_{xp} = 87.19$ lb, $F_{xb} = 12.81$ lb and $F_{xp} + F_{xb} = 100.00$ lb which equals $N_x H_p = 100.00$ lb.

When applying the load as shown in Figure 4, stresses in the plate have to account for the loads on the edge. The stress in the plate in this case is $\sigma_{yp} = 80.00$ psi and therefore $F_{yp} = 100.00$ lb, which exactly matches the total load applied along the edge.

Constant Curvature

All plate elements that include bending have to be able to represent the constant curvature state, $\kappa_x = w_{xx}$. This test is conducted following a description by Cook et al. (2002). To illustrate this test, one of the x direction an edge of the plate is clamped and a moment per length, m_y, is imposed along the opposite edge as shown in

Figure 5. The distributed moment is lumped in the same way as is done

with the forces. The rotations around the x-axis are constrained to be zero $(\theta_x = 0)$, at all exterior nodes in order to prevent curling of the edges. Assuming no rotation around the x-axis, the curvature in both the plate and beam can be computed from the stress using:

$$\sigma_x = \frac{Mc}{I} = \frac{EI\dfrac{\partial^2 w}{\partial x^2}c}{I} \tag{4}$$

Therefore,

$$E\kappa_x = E\frac{\partial^2 w}{\partial x^2} = \frac{\sigma_x}{c} \tag{5}$$

where σ_x: maximum stress in the x-direction; E: modulus of elasticity, 30×10^6 *psi*; κ_x: curvature in the x-direction; I: moment of inertia; and c: maximum offset from the neutral axis.

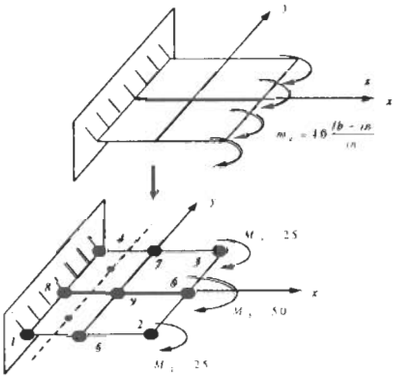

Figure 5 Constant moment applied on one side, constant curvature verified

A minor problem arises when performing this test due to the fact that the stresses in the plate are given only at the center of the plate, not at the clamped edge, while the stresses in the beam are given at the ends of the beam. Consequently, curvatures of the plates and of the beams are compared at a line parallel to the y-axis passing through the center of the two plates, and the beam, which lay closer to the clamped edge (shown in

Figure 5). The average of the stresses at the two nodes of the beams and the stress at the center of the plate are used. The curvature multiplied by the modulus of elasticity, E (same for the beam and plate) comes out to be:

$$E\left.\frac{\partial^2 w}{\partial x^2}\right|_{plate} = \frac{\sigma_x}{c_p} = \frac{908.53}{0.0625} = 14,536.44$$
$$E\left.\frac{\partial^2 w}{\partial x^2}\right|_{beam} = \frac{\sigma_{x1} + \sigma_{x2}}{2c_p} = \frac{3,808.02 + 3,521.132}{2 \times 0.25} = 14,658.30 \quad (6)$$

There is only a 0.8% difference in curvature at a midline through the plates and beam. Consequently, the constant curvature state is well preserved in the patch.

Modeling and Verification

The two models used in this study are a plate simply supported on two edges and stiffened on the two free edges with elastic beams, and a plate with four free edges, all stiffened by beams, and pinned supports on the corners. These two models are shown in
Figure 6.

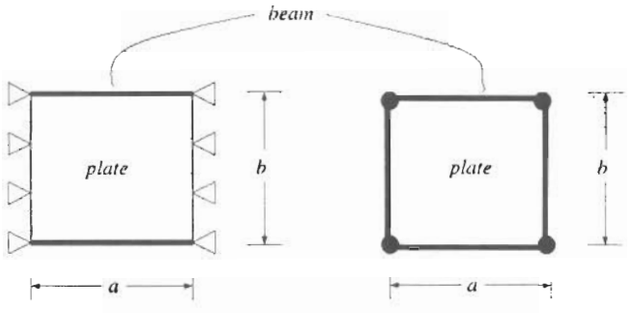

Figure 6 The Two models considered in the study

The objective is to verify the proposed finite element meshes by analyzing the plate using beam elements as stiffeners and comparing the results to the benchmark results from Timoshenko and Woinowsky-Krieger (1959) (shown in Appendix 1). In the verification process, the stiffener is also modeled with shell element and is referred as *shell-beam*. The *shell-beam* model is also compared to the benchmark model.

The material properties used both for the beam and the plate are the properties for typical steel: modulus of elasticity $E = 29 \times 10^6$ psi and Poisson's ratio $\nu = 0.3$. The aspect ratio (b/a) of the model ranges from 0.2/1 to 2/1. The beam stiffeners are on the two sides with length a, and are therefore tested both on longer and shorter edges of the plate.

Appendix 1: Analytical results from Timoshenko and Woinowsky-Krieger [1959]

Deflections and Bending Moments at the Center of a Uniformly Loaded Square Plate with Two Edges Simply Supported and the Other Two Supported by Elastic Beams ($\nu = 0.3$)

$\lambda = EI/aD$	W_{max}	$(M_x)_{max}$	$(M_y)_{max}$
∞	0.00406 qa^4/D	0.0479 qa^2	0.0479 qa^2
100	0.00409 qa^4/D	0.0481 qa^2	0.0477 qa^2
30	0.00416 qa^4/D	0.0486 qa^2	0.0473 qa^2
10	0.00434 qa^4/D	0.0500 qa^2	0.0465 qa^2
6	0.00454 qa^4/D	0.0514 qa^2	0.0455 qa^2
4	0.00472 qa^4/D	0.0528 qa^2	0.0447 qa^2
2	0.00529 qa^4/D	0.0571 qa^2	0.0419 qa^2
1	0.00624 qa^4/D	0.0643 qa^2	0.0376 qa^2
0.5	0.00756 qa^4/D	0.0744 qa^2	0.0315 qa^2
0	0.01309 qa^4/D	0.1225 qa^2	0.0271 qa^2

Deflections and Bending Moments in Uniformly Loaded Rectangular Plates with the Edges ($x = 0$ and $x = a$) Simply Supported and the Other Two Free ($\nu = 0.3$)

b/a	$x = a/2$ $y = 0$	$x = a/2$ $y = 0$	$x = a/2$ $y = 0$	$x = a/2$ $y = \pm b/2$	$x = a/2$ $y = \pm b/2$
	$w = \alpha_1 qa^4/D$ α_1	$M_x = \beta_1 qa^2$ β_1	$M_y = \beta_1 qa^2$ β_1	$w = \alpha_2 qa^4/D$ α_2	$M_y = \beta_2 qa^2$ β_2
0.5	0.01377	0.1235	0.0102	0.01443	0.1259
1.0	0.01309	0.1225	0.0271	0.01509	0.1318
2.0	0.01289	0.1235	0.0364	0.01521	0.1329
∞	0.01302	0.1250	0.0375	0.01522	0.1330

Deflections and Bending Moments in Uniformly Loaded Rectangular Plates with the Edges ($x = 0$ and $x = a$) Simply Supported and the Other Two Free ($\nu = 0.3$)

$\lambda = Et^3/aD$	$x = a/2,\ y = 0$	$x = a/2,\ y = 0$	$x = a/2,\ y = \pm b/2$
	$w = \alpha_1 qa^4/D$	$M_x = M_y = \beta_1 qa^2$	$M_x = \beta_2 qa^2$
	α_1	β_1	β_2
∞	0.00406	0.0460	0
100	0.00412	0.0462	
50	0.00418	0.0463	
25	0.00429	0.0467	0.0002
10	0.00464	0.0477	0.0024
5	0.00519	0.0494	0.0065
4	0.00546	0.0502	0.0085
3	0.00588	0.0515	0.0117
2	0. 00668	0.0539	0.0177
1	0.00873	0.0601	0.0332
0.5	0.01174	0.0691	0.0559
0	0.0257	0.1109	0.1527

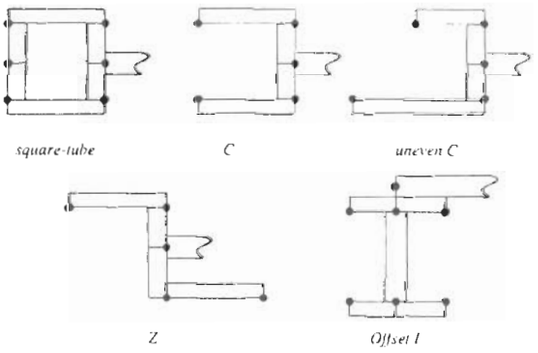

Figure 7 Shapes modeled in the study

Modeling Profiles with Shell Elements

When it deals with modeling the stiffeners with shell elements, five profiles (

Figure 7) are considered in this study. For the sake of simplicity, the shell elements used to model the beams are selected to be of the same thickness as the shell element in plate itself. All cross-sections are constructed to have the same moment of inertia, I_x based on the moment of inertia of the beam stiffener used to verify the model. I_y and J, however, are allowed to differ between different profiles. A mathematical package software Mathematica is used to calculate the dimensions of the profiles, keeping the moments of inertia the same while allowing the profiles

to be consisted of the same shell elements as the plate. The code can be found in Appendix 2. It is also noted that when applying loads to the plate supported by the offset I-beam, a rigid-link element has to be added in order to transfer the load to the beam model (Figure 8).

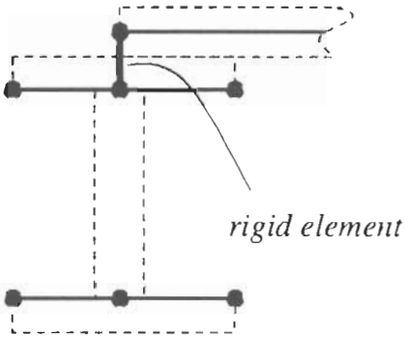

Figure 8 Rigid element added to transfer the load from the plate to the beam

Appendix 2: Mathematica Formulations

Analytical Results: Square Beam Properties

```
In[9]:= Clear[ EE, v, t, a, Ieq, DD, beq, λ, soll, wmax, Mxmax, Mymax, q ];

In[10]:= EE = 30. 10^6; v = 0.3; t = 0.125; a = 12.0;

In[11]:= DD = (EE t^3) / (12 (1 - v v)); λ = 4; Ieq = λ a DD / EE; beq = (Ieq 12)^0.25;

In[12]:= q = 10; wmax = 0.00472 q a^4 / DD; Mxmax = 0.0528 q a a; Mymax = 0.0447 q a a;

In[13]:= Print[TableForm[{{"D=", DD}, {"I=", Ieq}, {"b square =", beq}}]];
         D=              5365.73
         I=              0.00058516
         b square =      0.566542

In[14]:= Print[TableForm[{{"w=", wmax}, {"Mx=", Mxmax}, {"My =", Mymax}}]];
         w=      0.182406
         Mx=     76.032
         My =    64.368
```

Appendix 3: Mathematica Formulations (contimue)

C Beam and Z Beam Properties

```
In[32]:=
    Clear [h, w, th, tw, Ic, sol, Xc, Jc, Jz];

In[34]:= h = 2 w;  tw = th = t;

In[38]:= Ic = th (h - 2 tw) ^ 3 / 12 + 2 (w tw ^ 3 / 12 + w tw (h / 2 - tw / 2) ^ 2);

In[39]:= Xc = (th (h - 2 tw) th / 2 + w tw (w / 2) + w tw (w / 2)) / (th (h - 2 tw) + 2 w tw);

In[44]:= sol = Solve [{Ic == Ieq}, {w}];

In[45]:= w = sol [[3, 1, 2]];

    Jc = (h - 2 tw) th ((h - 2 tw) ^ 2 + th ^ 2) / 12 + h th (Xc - th / 2) ^ 2 +
       2 (w tw (w ^ 2 + tw ^ 2) / 12 + w tw ((Xc - w / 2) ^ 2 + (h / 2 - tw / 2) ^ 2));

    Jz = (h - 2 tw) th ((h - 2 tw) ^ 2 + th ^ 2) / 12 + 2 (w tw (w ^ 2 + tw ^ 2) / 12 +
          w tw ((w / 2 - th / 2) ^ 2 + (h / 2 - tw / 2) ^ 2));

    Print [TableForm [{{"H=", h}, {"W=", w}, {"tw =", tw}, {"th =", th}, {"X =", Xc},
        {"Jc =", Jc}, {"Jz =", Jz}}]];


    H=          0.706819
    W           0.353409
    tw          0.125
    th          0.125
    X           0.13187
    Jc          0.0101819
    Jz          0.0107315
```

Uneven C Beam Properties

```
In[16]:=
    Clear[h2, w2t, w2b, th2, tw2, Ic2, sol3, y, X2, Jc2];

In[17]:= h2 = w2t + w2b; w2b = 2 w2t; tw2 = th2 = t;

In[18]:= y = (th2 (h2 - 2 tw2) tw2 w2t (h2 / 2 - tw2 / 2) + (-1) tw2 w2b (h2 / 2 - tw2 / 2)) /
          (th2 (h2 - 2 tw2) + tw2 w2t + tw2 w2b);

In[19]:= Ic2 = th2 (h2 - 2 tw2) ^3 / 12 + th2 (h2 - 2 tw2) yy + (w2t tw2 ^ 3 / 12 + w2t tw2 (h2 / 2 - tw2 / 2 - y) ^2) +
        (w2b tw2 ^3 / 12 + w2b tw2 (h2 / 2 - tw2 / 2 + y) ^ 2);

    X2 = (th2 (h2 - 2 tw2) th2 / 2 + w2t tw2 (w2t / 2) +
         w2b tw2 (w2b / 2)) / (th2 (h2 - 2 tw2) + tw2 w2t + tw2 w2b);

In[21]:= sol3 = Solve[{Ic2 == Ieq}, {w2t}];

In[22]:= w2t = sol3[[3, 1, 2]];

In[25]:= Jc2 = (h2 - 2 tw2) th2 ((h2 - 2 tw2) ^ 2 + th2 ^ 2) / 12 + h2 th2 (X2 - th2 / 2) ^ 2 +
        (w2b tw2 (w2b^2 + tw2^2) / 12 + w2b tw2 ((X2 - w2b / 2) ^ 2 + (h2 / 2 - tw2 / 2 + y) ^2) +
        (w2t tw2 (w2t^2 + tw2^2) / 12 + w2t tw2 ((X2 - w2t / 2) ^2 + (h2 / 2 - tw2 / 2 - y) ^2));

    Print[TableForm[{{"H=", h2}, {"W top=", w2t}, {"W bottom=", w2b},
        {"tw =", tw2}, {"th =", th2}, {"X =", X2}, {"Y =", y}, {"Jc =", Jc2}}]];

    H           0.718973
    W top       0.239658
    W bottom    0.479316
    tw          0.125
    th          0.125
    X           0.185546
    Y           -0.0999144
    Jc          0.0109118
```

Appendix 4: Mathematica Formulations (continue)

Square Tube Beam Properties

```
In[31]:= Clear[Itube, btube, ttube, sol2, Jtube];

In[34]:= ttube = t;

In[35]:= Itube = 2 (ttube (btube - 2 ttube)^3 / 12 +
                 btube ttube^3 / 12 + btube ttube (btube / 2 - ttube / 2)^2);

In[36]:= sol2 = Solve[(Itube == Isq), {btube}];

In[37]:= btube = sol2[[3, 1, 2]];

In[38]:= Jtube = btube^4 / 6 - (btube - 2 ttube)^4 / 6;

In[40]:= Print[TableForm[{{"W =", btube}, {"t =", ttube}, {"J =", Jtube}}]];
         W          0.58268
         t          0.125
         J          0.0171703
```

Offset I Beam Properties

```
In[25]:= Clear[Itube, btube, ttube, sol2, Jtube];

In[26]:= ttube = t;

In[27]:= Itube = 2 (ttube (btube - 2 ttube)^3 / 12 +
                 btube ttube^3 / 12 + btube ttube (btube / 2 - ttube / 2)^2);

In[28]:= sol2 = Solve[(Itube == Isq), {btube}];

In[29]:= btube = sol2[[3, 1, 2]];

In[30]:= Jtube = btube^4 / 6 - (btube - 2 ttube)^4 / 6;

In[31]:= Print[TableForm[{{"W =", btube}, {"t =", ttube}, {"J =", Jtube}}]];
         W =        0.58268
         t =        0.125
         J =        0.0171703

In[32]:= Clear[Ii, hi, wi, twi, thi, sol4, Ji];

In[33]:= hi = 2 wi; twi = thi = t;

In[34]:= Ii = thi (hi - 2 twi)^3 / 12 + 2 (wi twi^3 / 12 + wi twi (hi / 2 - twi / 2)^2) +
          ((hi - 2 twi) thi + 2 wi twi) (hi / 2 + t / 2)^2;

In[35]:= wi = sol4[[3, 1, 2,]];

In[37]:= Ji = (hi - 2 twi) thi ((hi - twi)^2 + thi^2) / 12 +
          2 (w twi (w^2 + twi^2) / 12 + w twi (hi / 2 - twi / 2)^2);

In[38]:= Print[TableForm[{{"H =", hi}, {"W =", wi}, {"tw =", twi}, {"th =", thi}, {"J =", Ji}}]];

         H =        0.45294
         W =        0.22647
         tw =       0.125
         th =       0.125
         J =        0.00367046
```

Appendix 5 ***Analytical to FEM Comparison***

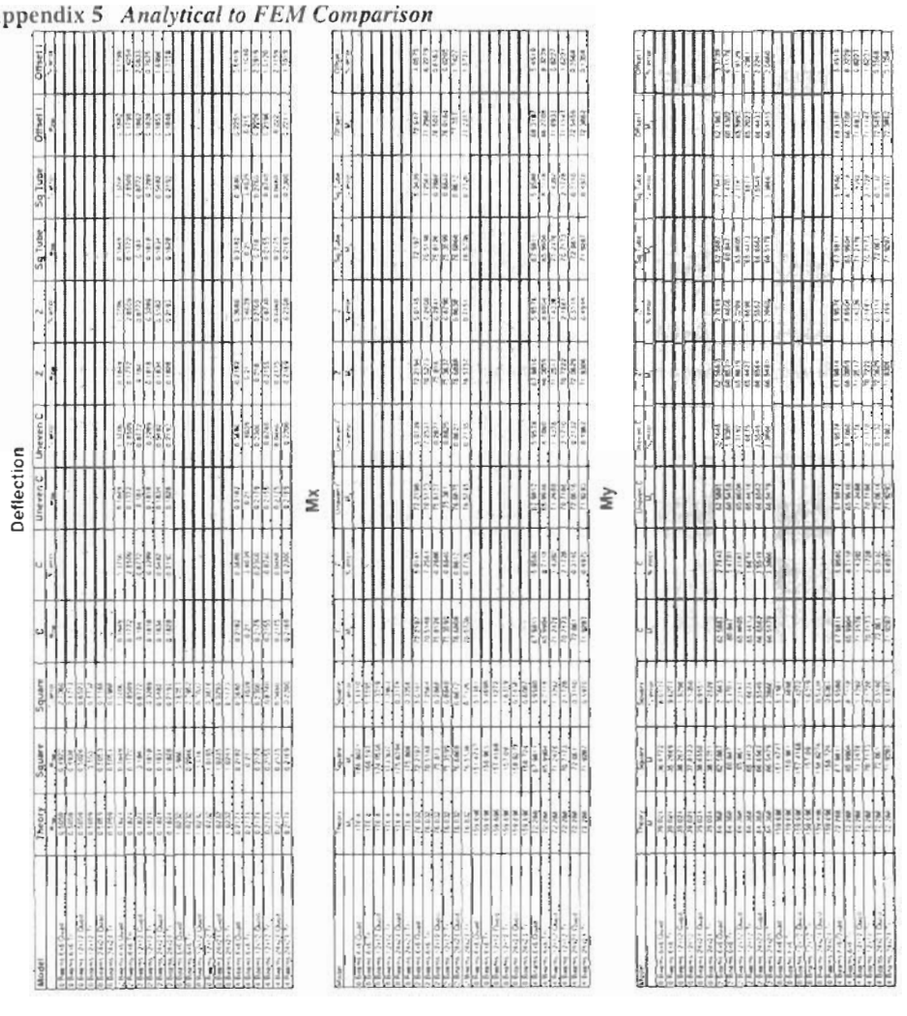

2 Edge Beam Size Ratio Comparison Between Analytical and FEM

Model	Theory	FEM			Model	Theory	FEM	
	w_{max}	w_{max}	% error			w_{max}	w_{max}	% error
0.5 to 1 6x6 Quad	8.5143	8.4164	-1.1498		2 to 1 6x6 Quad	0.4981	0.4867	-2.2887
0.5 to 1 6x6 Tri	8.5143	8.4299	-0.9913		2 to 1 6x6 Tri	0.4981	0.4862	-2.3891
0.5 to 1 12x12 Quad	8.5143	8.465	-0.5790		2 to 1 12x12 Quad	0.4981	0.4952	-0.5822
0.5 to 1 12x12 Tri	8.5143	8.4692	-0.5297		2 to 1 12x12 Tri	0.4981	0.4951	-0.6023
0.5 to 1 24x24 Quad	8.5143	8.4773	-0.4346		2 to 1 24x24 Quad	0.4981	0.4974	-0.1405
0.5 to 1 24x24 Tri	8.5143	8.4784	-0.4216		2 to 1 24x24 Tri	0.4981	0.4973	-0.1606
	Mx	Mx	% error			Mx	Mx	% error
0.5 to 1 6x6 Quad	711.36	703.7855	-1.1604		2 to 1 6x6 Quad	177.84	167.9172	-5.5796
0.5 to 1 6x6 Tri	711.36	702.495	-1.2462		2 to 1 6x6 Tri	177.84	167.701	-5.7012
0.5 to 1 12x12 Quad	711.36	709.9712	-0.1952		2 to 1 12x12 Quad	177.84	175.2944	-1.4314
0.5 to 1 12x12 Tri	711.36	709.75	-0.2263		2 to 1 12x12 Tri	177.84	175.211	-1.4783
0.5 to 1 24x24 Quad	711.36	711.6288	0.0378		2 to 1 24x24 Quad	177.84	177.137	-0.3953
0.5 to 1 24x24 Tri	711.36	711.572	0.0298		2 to 1 24x24 Tri	177.84	177.114	-0.4082
	Mx	Mx	% error			Mx	Mx	% error
0.5 to 1 6x6 Quad	69.12	66.8317	-3.3106		2 to 1 6x6 Quad	52.416	49.6328	-5.3098
0.5 to 1 6x6 Tri	69.12	64.7467	-6.3271		2 to 1 6x6 Tri	52.416	49.2601	-6.0209
0.5 to 1 12x12 Quad	69.12	68.7287	-0.5661		2 to 1 12x12 Quad	52.416	51.6948	-1.3759
0.5 to 1 12x12 Tri	69.12	68.029	-1.5784		2 to 1 12x12 Tri	52.416	51.5793	-1.5963
0.5 to 1 24x24 Quad	69.12	69.2412	0.1753		2 to 1 24x24 Quad	52.416	52.2005	-0.4111
0.5 to 1 24x24 Tri	69.12	69.0565	-0.0919		2 to 1 24x24 Tri	52.416	52.1704	-0.4686

Model Verification

The comparison of the models is performed by investigating the deflection, w as well as the moments, both around x-axis and y-axis, at the center of the plate. For the sake of conciseness, only results from the deflection comparisons are presented here as shown in **Table 1**, **Table 2**,

Table 3, and ผิดพลาด! ไม่พบแหล่งการอ้างอิง but more comprehensive results can be found in **Appendix 5**. The plates are loaded with a constant pressure load and the results are compared with the benchmark solutions from Timoshenko and Woinowsky-Krieger (1959). Clearly, the results show that the error decreases with the finer mesh, which is consistent with the results from the patch tests. Furthermore, the finite element analysis tends to underestimate the center deflection (percentages shown with minus sign), which is typical for the displacement-based elements.

Analysis

Static Analysis

Unfortunately, no analytical result is available to completely verify the shell-beam stiffeners. This is due to the fact that available analytical results do not deal with the torsional stiffness of the stiffeners. Also, the analytical results have the centroidal axis of the beams passing through the edge of the plate, while the proposed profiles have the shell-beam edge attached to the edge of the plate.

However, based on the excellent results given by the element model with beam stiffeners, it is confident to use the model with and without torsional stiffness as the benchmark model for comparisons. In the tables shown below, J and No-J refer to torsional stiffness being included or excluded in the beam.

It is clearly seen in ผิดพลาด! ไม่พบแหล่งการอ้างอิง that the square tube profile has consistently larger percent difference than other profiles unless torsional stiffness is added to the beam model. This indicates importance of including the torsional stiffness in the stiffeners if beams are used to model them and the real stiffener is a closed cross-section. This is in agreement with the well-known fact that closed cross-sections resist torsion much better than opened cross-sections. It can also be seen that the addition of the torsional stiffness, J to the beam element produces a larger percent difference with the shell-beam model for opened cross-sections.

Frequency Analysis

As in the static analysis, no analytical solution is available to verify the shell stiffeners. Consequently, the beam model is used as a benchmark model. For the sake of the brevity, only the first (bending) and second (torsion) modes of vibration are represented in

Table 6 and **Table 7**, respectively.

The square tube cross-section has a large percent difference in the second mode for the models with the beams on the longer edges. This is believed to be a result of the torsional stiffness automatically accounted by the shell-beam model since the second mode is a plate-twisting mode.

Table 1 Difference in unstiffened plate with two sides simply supports

Element Type	Num. of Elements	% Error
Quad-4	6 × 6	-2.70
Quad-4	12 × 12	-0.65
Quad-4	24 × 24	-0.12
Triangular	6 × 6	-2.43
Triangular	12 × 12	-0.57
Triangular	24 × 24	-0.10

Table 2 Difference where two sides are simply supported and two stiffened

Element Type	Num. of Elements	Square % Error	C % Error	Uneven C % Error	Z % Error	Square-Tube % Error	Offset I % Error
Quad-4	6 × 6	-1.35	-1.35	-1.35	-1.35	-1.35	-3.15
Quad-4	12 × 12	-0.88	-0.88	-0.88	-0.89	-0.88	-2.07
Quad-4	24 × 24	-0.55	-0.55	-0.55	-0.55	-0.55	-1.67
Triangular	6 × 6	-2.87	-2.87	-2.87	-2.85	-2.87	-1.43
Triangular	12 × 12	-0.33	-0.33	-0.33	-0.32	-0.33	-0.79
Triangular	24 × 24	-0.23	-0.23	-0.23	-0.23	-0.23	-1.32

Table 3 Difference in unstiffened plate with four sides free and corners pinned

Element Type	Num. of Elements	% Error
Quad-4	6 × 6	-3.63
Quad-4	12 × 12	-0.70
Quad-4	24 × 24	-0.03
Triangular	6 × 6	-2.80
Triangular	12 × 12	-0.36
Triangular	24 × 24	-0.11

Table 4 Difference where all four sides are stiffened and corners are pinned

Element Type	Num. of Elements	Square % Error	C % Error	Uneven C % Error	Z % Error	Square-Tube % Error	Offset I % Error
Quad-4	6 × 6	-0.36	-0.36	-0.36	-0.36	-0.36	-2.12
Quad-4	12 × 12	-0.26	-0.26	-0.26	-0.26	-0.26	-2.40
Quad-4	24 × 24	-0.06	-0.06	-0.06	-0.06	-0.06	-0.36
Triangular	6 × 6	-3.41	-3.41	-3.40	-3.38	-3.41	-1.71
Triangular	12 × 12	-0.87	-0.87	-0.87	-0.86	-0.87	-1.02
Triangular	24 × 24	-0.23	-0.23	-0.23	-0.23	-0.23	-1.09

Table 5 Center deflection comparison between shell-beam and beam

b/a	0.2/1	0.2/1	2/1	2/1
Section Profile	No-J % Diff	J % Diff	No-J % Diff	J % Diff
C	-0.1140	-0.2007	-5.9762	14.8342
Uneven C	-0.0974	-0.1896	-6.4599	14.9851
Z	-0.4688	-0.5570	-3.4440	18.1438
Square Tube	-0.1162	**-0.0108**	-14.5172	6.0775
Offset I	0.0440	0.0925	-2.0390	13.1698

Table 6 First mode frequency comparison: shell-beam to beam

b/a	0.2/1	0.2/1	1/1	1/1
Section Profile	No-J % Diff	J % Diff	No-J % Diff	J % Diff
C	0.0549	0.0459	3.0106	-6.4129
Uneven C	7.0612	7.0536	10.5378	0.0420
Z	7.2804	7.2707	8.6243	-1.4120
Square Tube	7.1204	7.0984	14.6371	3.8750
Offset I	-0.0470	-0.0513	0.9527	-5.9525

Table 7 Second mode frequency comparison: shell-beam to beam

b/a	0.2/1	0.2/1	1/1	1/1
Section Profile	No-J % Diff	J % Diff	No-J % Diff	J % Diff
C	4.4887	-28.5137	-0.7796	-1.2600
Uneven C	11.6977	-24.2005	6.0050	5.3787
Z	12.6193	-23.6803	5.7926	5.1970
Square Tube	58.9635	-1.9980	5.7404	5.7323
Offset I	1.7385	-17.2766	-0.9829	-1.5615

Conclusion

FEAP (Taylor, 1998) is capable of matching theoretical results closely with a fine enough grid, achieving 0.12 % and 0.03 % errors with 24×24 mesh for the plate with two and four stiffeners, respectively.

Depending on the number of elements used, there is a good relationship between beam elements with no torsional stiffness and opened profile shell-beams. This confirms how weakly opened cross-sections can resist torsional loads.

Closed profile shell-beam seem to have a major effect (possibly due to torsional stiffness) on the frequencies of twisting modes of a plate stiffened with beam along the longer edge.

Mixing plate and beam elements in FEAP (Taylor, 1998) is highly recommended due to the modeling and computational costs saved. Cares, however, have to be taken with the torsional stiffness of the beam element accounting for the cross-sectional shape being considered.

References

Bazeley, G.P., Cheung, Y.K., Irons, B.M., and Zienkiewicz, O.C.1966. Triangular Elements in Plate Bending: Conforming and Nonconforming solutions. **Conference on Matrix Methods in**

Structural Mechanics. Air Force Institute of Technology, Dayton: Ohio, USA: 547-584.

Cook, R.D., Malkus, D.S., Plesha, M.E., and Witt, R.J. 2002. Concepts and Applications of Finite Element Analysis. 4th ed. USA: **John Wiley**.

Laura, P.A.A. and Romanelli (1974) "Vibrations of Rectangular Plates Elastically Restrained against Rotation along All Edges and Subjected to a Biaxial State of Stress". **Journal of Sound and Vibration**.37,3: 367-377.

Leissa A.W., Laura, P.A.A., and Gutierrez, R.H. 1980. "Vibrations of Rectangular Plates with Nonuniform Elastic Edge Supports". **ASME Journal of Applied Mechanics**. 47: 891-895.

Taylor, R.L. 1998. FEAP: A Finite Element Analysis Program. Version 7.1. Department of Civil and Environmental Engineering, **University of California, Berkeley**. USA.

Timoshenko, S. and Woinowsky-Krieger, S. 1959. Theory of Plates and Shells. 2nd. Ed. USA.: **McGraw-Hill**.